ChemSusChem

Research Article
doi.org/10.1002/cssc.202301050

Chemistry Europe
European Chemical Societies Publishing

www.chemsuschem.org

Highly efficient electrochemical ammonia synthesis via nitrate reduction over metallic Cu phase coupling sulfion oxidation

Zhi Wang[+],[a, b] Na Zhou[+],[a, b] Jiazhi Wang[+],[a, b] Depeng Wang,[a, b] Jianrong Zeng,[c, d] Haixia Zhong,*[a, b] and Xinbo Zhang*[a, b]

Electrochemical nitrate reduction reaction (NO_3RR) is a promising technology for ammonia production and denitrification of wastewater. Its application is seriously restricted by the development of the highly active and selective electrocatalyst and a rational electrolysis system. Here, we constructed an efficient electrochemical ammonia production process via nitrate reduction on the metallic Cu electrocatalyst when coupled with anodic sulfion oxidation reaction (SOR). The synthesized Cu catalyst delivers an excellent NH_3 Faradaic efficiency of 96.0% and a NH_3 yield of 0.391 mmol h^{-1} cm^{-2} at −0.2 V vs. reversible hydrogen electrode, which mainly stem from the more favorable conversion of NO_2^- to NH_3 on Cu^0. Importantly, the well-designed electrolysis system with cathodic NO_3RR and anodic SOR achieves a dramatically reduced cell voltage of 0.8 V at 50 mA cm^{-2} in comparison with the one with anodic oxygen evolution reaction (OER) of 1.9 V. This work presents an effective strategy for the energy-saving ammonia production via constructing effective nitrate reduction catalyst and replacing the OER with SOR while removing the pollutants including nitrate and sulfion.

Introduction

Ammonia (NH_3), as an indispensable feedstock for fertilizers and pharmaceuticals production, is one of the most productive chemicals.[1] Meanwhile, due to its high hydrogen content (17.8 wt.%) and relatively easy liquefaction conditions (~10 bar at room temperature or −33 °C at atmospheric pressure), NH_3 is a potential hydrogen carrier and carbon-free fuel.[2] Currently, the mature industrial NH_3 synthesis depends on the energy-intensive Haber-Bosch (H-B) process alongside massive CO_2 emission.[3] Electrochemical N_2/NO_3^- reduction reaction (NRR/NO_3RR) to ammonia under mild conditions using renewable electricity is increasingly being investigated as an attractive alternative.[4] Nevertheless, on account of the chemical inertness of N_2, poor NH_3 yield and Faradaic efficiency (FE) have been achieved via NRR.[5] In contrast, owing to low dissociation energy of N=O bond, electrochemical NO_3RR is more kinetically favorable.[6] Nitrate can be obtained from agricultural runoff, industrial wastewater and N_2 via plasma treatments.[7] Therefore, NO_3RR offers a promising alternative for large-scale ammonia production and the denitrification of wastewater, wherein efficient electrocatalysts and a suitable electrolysis system are crucial.

Cu-based catalysts have been widely used for NO_3RR to ammonia as a result of its moderate adsorption energy of intermediates and effective suppression of hydrogen evolution.[8] However, the sluggish kinetics of NO_2^- intermediates conversion to NH_3 on Cu at low overpotential will inevitably result in the unsatisfactory ammonia production with superabundant NO_2^- byproducts and high energy input.[8] Additionally, the effective active sites of Cu-based catalysts are still not clear owing to the unstable oxidation state and structure.[9] To solve these problems, morphology, defect, crystal plane and interface designs have been developed.[10] For example, Jiang et al. constructed the Cu-Al_2O_3 interface to stabilize the $Cu^{\delta+}$, which was accounted for the robust NO_3RR performance.[11] Conversely, Zhou et al. proposed that Cu^0 is the real active phase for the highly selective NO_3RR to NH_3.[9] Based on our density functional theory (DFT) calculations, we found that the NO_3^- adsorption on Cu_2O is stronger than on Cu and the NH_3 desorption on Cu is far more efficient than on Cu_2O (Figures 1 and S1). It means that the stable Cu^0 at the reduction potential can achieve a more favorable conversion of NO_3^- to NH_3 than the unstable Cu^+. Thus, developing metallic Cu

[a] Z. Wang,[+] N. Zhou,[+] Dr. J. Wang,[+] D. Wang, Prof. H. Zhong, Prof. X. Zhang
State Key Laboratory of Rare Earth Resource Utilization, Changchun Institute of Applied Chemistry
Chinese Academy of Sciences
5625 Renmin Street, Changchun 130022, China
E-mail: hxzhong@ciac.ac.cn
xbzhang@ciac.ac.cn

[b] Z. Wang,[+] N. Zhou,[+] Dr. J. Wang,[+] D. Wang, Prof. H. Zhong, Prof. X. Zhang
School of Applied Chemistry and Engineering
University of Science and Technology of China
96 Jinzhai Street, Hefei 230026, China

[c] Prof. J. Zeng
Shanghai Synchrotron Radiation Facility, Shanghai Advanced Research Institute
Chinese Academy of Sciences
239 Zhangheng Street, Shanghai 201204, China

[d] Prof. J. Zeng
Shanghai Institute of Applied Physics
Chinese Academy of Sciences
2019 Jialuogong Street, Shanghai 201800, China

[+] These authors contributed equally.

Supporting information for this article is available on the WWW under https://doi.org/10.1002/cssc.202301050

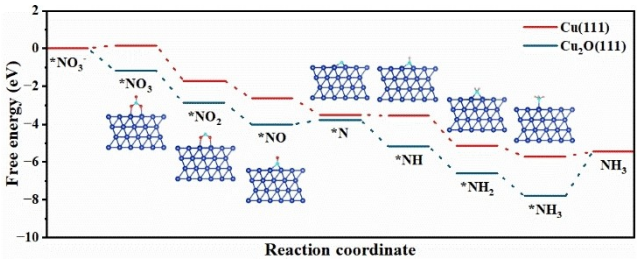

Figure 1. The calculated Gibbs free energy diagrams for NO_3^--to-NH_3 conversion on Cu and Cu_2O catalyst. The blue, red, cyan and pink balls represent copper, oxygen, nitrogen and hydrogen atoms, respectively.

catalysts is desirable for NO_3RR to ammonia yet very challenging.

In addition to the ungratified NO_3RR catalyst design, the energy-efficient ammonia production is also restricted by anodic oxygen evolution reaction (OER) due to its high potential (0.401 V vs. SHE, pH = 14) and the slow multiple proton-coupled electron-transfer kinetics.[12] It is necessary to substitute OER with more favorable anodic oxidation reaction for highly efficient ammonia production with reduced cell voltage, such as sulfion oxidation reaction (SOR) with lower oxidation potential (S^{2-}-$2e^-$ = S, −0.48 V vs. SHE, pH = 14).[13] Moreover, this electrochemical SOR also affords an sustainable avenue to convert the toxic pollutants (e.g. H_2S or S^{2-}) from oil refineries and nature-gas extraction industries to harmless elemental sulfur.[14] Therefore, the system coupling NO_3RR with SOR is attractive for the lower-cost and high-efficiency NH_3 production and pollutant degradation.

Herein, we demonstrated that the selective and low-energy NH_3 synthesis can be built through the promoted NO_3^- reduction on the cathodic metallic Cu catalyst and replacing the traditional OER with SOR. Density functional theory (DFT) calculations show that the NO_2^- conversion to NH_3 on metallic Cu phase is more favorable than that on Cu_2O. The synthesized metallic Cu electrocatalyst presents a NH_3 Faradaic efficiency of 96.0% and a NH_3 yield of 0.391 mmol h^{-1} cm^{-2} at a low potential of −0.2 V vs. RHE, which is better than these Cu_2O catalysts. Coupling NO_3RR with SOR, NH_3 production was proceed at an ultralow cell voltage of 1.2 V at the current density of around 85 mA cm^{-2} in two-electrode electrolysis system. A notable reduction of 50% in the cell voltage is observed for the NO_3RR-SOR system (1.2 V) with respect to the NO_3RR-OER one (2.387 V). Our findings provide a general strategy for developing metal Cu catalyst and energy-saving ammonia synthesis process as well.

Results and Discussion

On basis of DFT results, metal Cu particles were synthesized for electrocatalytic nitrate reduction to ammonia. To alleviate the formation of oxide phases, a chemical reduction and precipitation process was rapidly finished to synthesize the Cu catalysts (CR-Cu). As shown by the transmission electron microscopy (TEM) image, the selected area electron diffraction (SAED) pattern and the scanning electron microscopy (SEM) image, CR-Cu is polycrystalline with an average particle size of ~28.8 nm (Figures 2a and S2). Clear lattice spacing of 2.08 Å is found in the high-resolution transmission electron microscopy (HRTEM) image of CR-Cu, which corresponds to Cu(111) (Figure 2b). Through the scanning transmission electron microscopy-energy dispersive X-ray spectroscopy (STEM-EDX) elemental mapping analysis, trace surface oxygen element despite Cu element was detected for CR-Cu (Figure 2c–e), which is likely associated with the surface oxidation of Cu nanoparticles.

However, the X-ray diffraction (XRD) patterns illustrate no obvious characteristic peaks of oxide phases for CR-Cu compared with the commercial Cu particles with minimal Cu_2O peaks at 36.6°, 42.5° and 61.6° (Figure 3a). Nevertheless, the X-

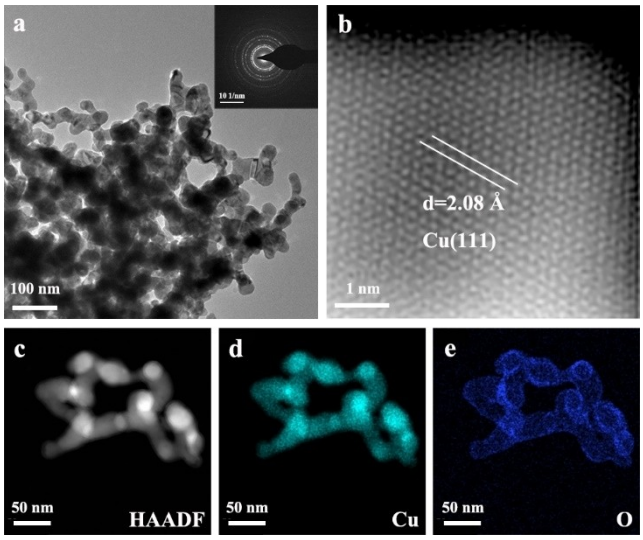

Figure 2. (a) TEM image and the corresponding SAED pattern (insert) of CR-Cu. (b) HRTEM image of CR-Cu. (c) HAADF-STEM image and EDX elemental mapping of Cu (d) and O (e) elements in CR-Cu.

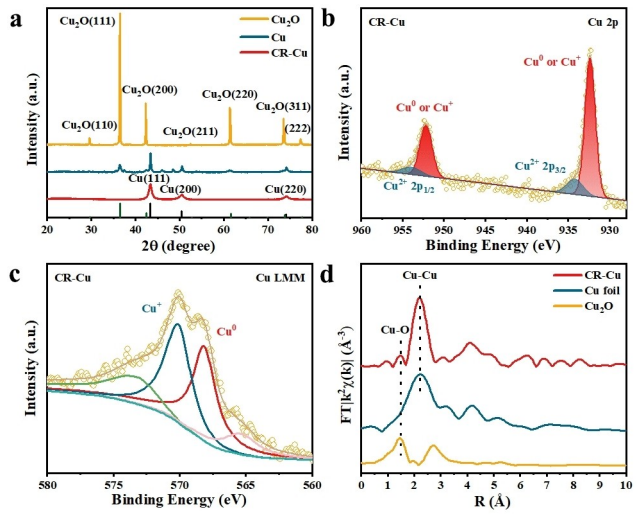

Figure 3. (a) XRD patterns of Cu_2O, Cu and CR-Cu. (b) Cu 2p XPS spectra and (c) Cu LMM AES spectra of CR-Cu. (d) FT-EXAFS spectra of CR-Cu, Cu foil, and Cu_2O.

ray photoelectron spectroscopy (XPS) spectrum indicates the existence of Cu and O element for CR-Cu (Figures S3), which is consisted with the EDX analysis. Figure 3b shows the high-resolution Cu 2p spectrum of CR-Cu. Two set of peaks at 932.6 and 952.3 eV are assigned to Cu $2p_{3/2}$ and Cu $2p_{1/2}$, respectively. The according deconvoluted spectrum indicates the existence of Cu^0/Cu^+ of CR-Cu.[15] The high-resolution Cu LMM Auger electron spectroscopy (AES) spectra of CR-Cu further reflect that the content of external Cu^+ to Cu^0 and certify the presence of amorphous oxide phases, which cannot be detected by XRD (Figure 3c).[16] In addition, X-ray absorption spectroscopy (XAS) analyses were performed to further investigate the chemical state of the Cu atoms in the CR-Cu sample. As shown in Figure S4, the Cu K-edge X-ray absorption near-edge structure (XANES) spectra indicate that CR-Cu exhibits a similar typical Cu^0 peak compared to the reference Cu foil, which is different from the Cu_2O.[17] Notably, the minimal positive peak shift of CR-Cu compared to Cu foil reference was due to the partial oxidation of CR-Cu, which is consisted with the XPS results. The Fourier-transformed extended X-ray absorption fine structure (FT-EXAFS) in Figure 3d further elucidates the Cu-O and Cu-Cu configuration of CR-Cu.[16a] It is thus clear that CR-Cu with slightly oxidation was successfully synthesized.[18]

Regarding the presence of surface Cu-based oxides, CR-Cu was further treated by an electrochemical reduction method (abbreviated as ER-Cu, Figures S5 and S6).[9] To evaluate the NO_3RR performance of these Cu catalysts, chronoamperometry tests were conducted in 1 M KOH electrolyte with 0.1 M KNO_3. The products were detected by UV-vis photometer and ion chromatography (Figures S7 and S8). As shown in Figure 4a, ER-Cu exhibits higher NH_3 selectivity with larger Faradaic efficiency than CR-Cu and Cu_2O over the overall applied potentials. At −0.2 V vs. RHE, ER-Cu reaches a maximum NH_3 Faradaic efficiency up to 96.0%, superior to CR-Cu (81.5%) and Cu_2O (76.3%), as well as other similar Cu-based electrocatalyst (Figure S9 and Table S1). Accordingly, the calculated molar concentration ratios of NH_3 to NO_2^- for these samples are shown in Figure 4b. Upon increasing the applied reduction potentials, the ratio of NH_3 for all these samples increases due to the accelerated reduction of NO_2^- to NH_3 at high overpotential. Larger molar ratio of NH_3 to NO_2^- is observed on ER-Cu compared to CR-Cu and Cu_2O. Thus, the conversion of NO_2^- to NH_3 on metallic Cu phase is more favorable, which is consisted with the DFT calculations. The NH_3 yield for all the samples increases upon varying the applied potential from 0 to −0.3 V vs. RHE as well. The NH_3 yield for ER-Cu was calculated to be 0.391 mmol h^{-1} cm^{-2} at −0.2 V vs. RHE, which outcompetes CR-Cu (0.278 mmol h^{-1} cm^{-2}) and Cu_2O (0.146 mmol h^{-1} cm^{-2}) (Figure 4c). To prove that NH_3 originates from specific reactants, isotope labelling experiments were conducted using $^{15}NO_3^-$ and $^{14}NO_3^-$ as the nitrogen source, respectively. Two typical peaks of $^{15}NH_4^+$ or three typical peaks of $^{14}NH_4^+$ are individually observed in the ^1H NMR spectra of the electrolyte using $^{15}NO_3^-$ and $^{14}NO_3^-$, confirming that NO_3^- in the electrolyte is the nitrogen source (Figure 4d) for ammonia generation.[19]

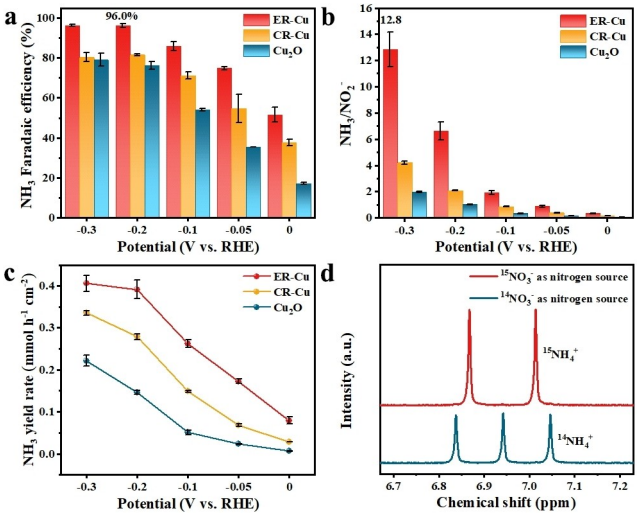

Figure 4. (a) Faradaic efficiency of NH_3 at various potentials for ER-Cu, CR-Cu and Cu_2O. (b) Molar concentration ratio of NH_3 to NO_2^- at different potentials for ER-Cu, CR-Cu and Cu_2O. (c) Yield rate of NH_3 at various potentials for ER-Cu, CR-Cu and Cu_2O. (d) ^1H NMR spectra of $^{15}NH_4^+$ and $^{14}NH_4^+$ produced after NO_3RR over ER-Cu electrode using $^{15}NO_3^-$ and $^{14}NO_3^-$ as the nitrogen source, respectively.

For the practical NH_3 production, low energy input is necessary. Given that high potential is required to drive OER, anodic SOR is considered to reduce the overall electrolysis cell voltage. CR-Cu after the electrochemically sulfurization (ES-Cu) was not used for SOR due to its unsatisfactory catalytic performance (Figure S14). Here, the typically active anodic oxidation electrocatalyst, such as Ni/Fe hydroxides on Ni foam, was chosen to replace the Pt counter electrode considering the high catalytic performance of Ni/Fe sites toward the anodic oxidation reactions.[20] The anode with excellent SOR activity was prepared by doping S into the typically OER active Ni/Fe hydroxide [S-(Ni,Fe)O_xH_y] on Ni foam, as manifested by XRD, SEM, SAED, TEM-EDX, XPS spectra and linear sweep voltammetry (see detailed discussion in Supporting Information, Figures S10–14).[21] The polarization curves (Figure 5a) uncover that the onset potentials of SOR and OER are 0.288 and 1.366 V vs. RHE, respectively. Such a low onset potential of SOR is undoubtedly conducive to reducing the energy demand of NH_3 production. The long-term stability of SOR on S-(Ni,Fe)O_xH_y electrode was tested at 100 mA cm^{-2} for 24 h (Figure S15). The activity of the catalyst remains stable, evidencing the good stability of the S-doped Ni/Fe hydroxide. The UV-vis spectra of the electrolyte during the 8 h SOR test at 100 mA cm^{-2} showcase the absorption peaks at 300 and 370 nm, certifying the formation of polysulfides products (S_x^{2-}, $2 \leq x \leq 4$) (Figure S16a).[22] After 8-hours SOR test, the electrolyte turned brown and the polysulfides in electrolyte were treated with acid to obtain the pale-yellow S powder, which was indicated by XRD analysis (Figure S16b).[23] Thus, substituting the OER with SOR is feasible for reducing the energy input for the electrochemical NH_3 synthesis.

Two-electrode systems of the cathodic NO_3RR with anodic SOR or OER were further used for NH_3 synthesis. The polarization curves suggest that the cell voltages of 1.2 and 2.387 V are severally required to reach the same current density of

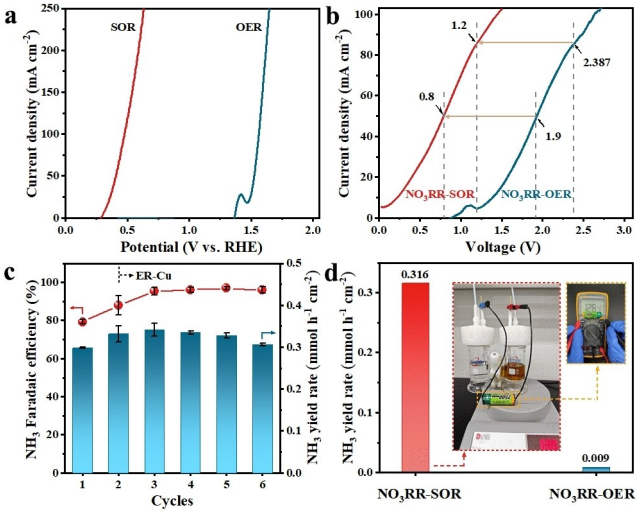

Figure 5. (a) Polarization curves of SOR on the S-(Ni,Fe)O_xH_y electrode and polarization curves of OER on the (Ni,Fe)O_xH_y electrode. (b) Polarization curves of the two-electrode NO_3RR-SOR and NO_3RR-OER systems. (c) Cyclability test of the two-electrode NO_3RR-SOR system at 1.2 V with CR-Cu as cathode and S-(Ni,Fe)O_xH_y as anode. (d) NH_3 yield rate of two-electrode systems driven by a commercial battery with the nominal voltage of 1.2 V and the photo of corresponding NO_3RR-SOR system.

around 85 mA cm^{-2} for the NO_3RR-SOR and NO_3RR-OER system (Figure 5b). The reduction of 50% about cell voltage corresponds to the significant energy saving. The cycling stability test of two-electrode NO_3RR-SOR system with cathodic metallic Cu catalyst was carried out (Figure 5c) at the cell voltage of 1.2 V. After the second cycle, the Faradaic efficiency of NH_3 maintains around 95%, which is associated with the conversion of CR-Cu to ER-Cu and more favorable ammonia generation process. Meanwhile, the characterizations of ER-Cu after the long-term durability test are shown in Figures S17 and S18. Results illustrate the maintained structure and morphology of ER-Cu, accompany with slight particle fragmentation and reaggregation after the long-term durability test, corroborating the good stability of the metallic Cu catalyst. More importantly, the efficient ammonia production can be driven by a commercial battery with the nominal voltage of 1.2 V (Figures 5d and S19). And the NH_3 yield rate is 0.316 mmol h^{-1} cm^{-2} for this NO_3RR-SOR system. Meanwhile, only negligible amount of NH_3 was generated in the NO_3RR-OER system driven by this commercial battery.

Conclusions

In conclusion, we attested to the efficient nitrate reduction to NH_3 on metallic Cu electrocatalyst and realized an energy-saving ammonia production system of cathodic NO_3RR and anodic SOR. Due to the more favorable conversion NO_2^- to NH_3, the metallic Cu catalyst synthesized by a chemical and electrochemical reduction approach achieves a high NH_3 Faradaic efficiency of 96.0% and a NH_3 yield of 0.391 mmol h^{-1} cm^{-2} at a low potential of −0.2 V vs. RHE. By virtue of the lower onset potential of SOR compared to OER, the efficient NH_3 production via NO_3RR integrated with anodic SOR was obtained, presenting a NH_3 Faradaic efficiency of around 95% at a smaller cell voltage of 1.2 V. This signifies a 50% decrease in cell voltage relative to the NO_3RR-OER system. Our findings will offer guidance on the rational design of nitrate reduction catalysts and the effective strategy for energy-saving electrolysis process via utilizing the more thermodynamically and kinetically favorable anodic reaction, as well as a sustainable route for the removal of water pollutants.

Supporting Information

The authors have cited additional references within the Supporting Information (Ref. [24–29]).

Acknowledgements

This work was supported by National Key R&D Program of China (2021YFB4000402), the National Natural Science Foundation of China (52071311, 52273277, 52072362), Jilin Province Science and Technology Development Plan Funding Project (20220201112GX) and Youth Innovation Promotion Association CAS (2020230 and 2021223). H.X.Z. acknowledges funding from National Natural Science Foundation of China Outstanding Youth Science Foundation of China (Overseas). These authors thank the staff of beamline BL13SSW at Shanghai Synchrotron Radiation Facility for experiments supports.

Conflict of Interests

The authors declare no conflict of interest.

Data Availability Statement

The data that support the findings of this study are available from the corresponding author upon reasonable request.

Keywords: nitrate reduction · ammonia production · metallic Cu electrocatalyst · sulfion oxidation · energy-saving

[1] a) V. Rosca, M. Duca, M. T. de Groot, M. T. M. Koper, *Chem. Rev.* **2009**, *109*, 2209–2244; b) T. Ren, Z. Yu, H. Yu, K. Deng, Z. Wang, X. Li, H. Wang, L. Wang, Y. Xu, *Appl. Catal. B* **2022**, *318*, 121805.
[2] a) Y. Gao, Q. Xia, L. Hao, A. W. Robertson, Z. Sun, *ACS Sustainable Chem. Eng.* **2022**, *10*, 1316–1322; b) D. R. MacFarlane, P. V. Cherepanov, J. Choi, B. H. R. Suryanto, R. Y. Hodgetts, J. M. Bakker, F. M. F. Vallana, A. N. Simonov, *Joule* **2020**, *4*, 1186–1205.
[3] N. C. Kani, N. H. L. Nguyen, K. Markel, R. R. Bhawnani, B. Shindel, K. Sharma, S. Kim, V. P. Dravid, V. Berry, J. A. Gauthier, M. R. Singh, *Adv. Energy Mater.* **2023**, *13*, 2204236.
[4] J. Li, G. M. Zhan, J. H. Yang, F. J. Quan, C. L. Mao, Y. Liu, B. Wang, F. C. Lei, L. J. Li, A. W. M. Chan, L. P. Xu, Y. B. Shi, Y. Du, W. C. Hao, P. K. Wong, J. F. Wang, S. X. Dou, L. Z. Zhang, J. C. Yu, *J. Am. Chem. Soc.* **2020**, *142*, 7036–7046.
[5] a) Y. Wang, H. Li, W. Zhou, X. Zhang, B. Zhang, Y. Yu, *Angew. Chem. Int. Ed.* **2022**, *61*, e202202604; b) Z. Deng, J. Liang, Q. Liu, C. Ma, L. Xie, L.

Yue, Y. Ren, T. Li, Y. Luo, N. Li, B. Tang, A. Ali Alshehri, I. Shakir, P. O. Agboola, S. Yan, B. Zheng, J. Du, Q. Kong, X. Sun, *Chem. Eng. J.* **2022**, *435*, 135104.
[6] F. Lv, M. Z. Sun, Y. P. Hu, J. Xu, W. Huang, N. Han, B. L. Huang, Y. G. Li, *Energy Environ. Sci.* **2023**, *16*, 201–209.
[7] a) Q. Gao, H. S. Pillai, Y. Huang, S. K. Liu, Q. M. Mu, X. Han, Z. H. Yan, H. Zhou, Q. He, H. L. Xin, H. Y. Zhu, *Nat. Commun.* **2022**, *13*, 2338; b) X. Zhang, Y. T. Wang, C. B. Liu, Y. F. Yu, S. Y. Lu, B. Zhang, *Chem. Eng. J.* **2021**, *403*, 126269.
[8] a) H. M. Liu, X. Y. Lang, C. Zhu, J. Timoshenko, M. Rüscher, L. C. Bai, N. Guijarro, H. B. Yin, Y. Peng, J. H. Li, Z. Liu, W. C. Wang, B. Roldan Cuenya, J. S. Luo, *Angew. Chem. Int. Ed.* **2022**, *61*, e202202556; b) W. D. Wen, P. Yan, W. P. Sun, Y. T. Zhou, X. Y. Yu, *Adv. Funct. Mater.* **2023**, *33*, 2212236.
[9] N. Zhou, Z. Wang, N. Zhang, D. Bao, H. X. Zhong, X. B. Zhang, *ACS Catal.* **2023**, *13*, 7529–7537.
[10] a) X. B. Fu, X. G. Zhao, X. B. Hu, K. He, Y. N. Yu, T. Li, Q. Tu, X. Qian, Q. Yue, M. R. Wasielewski, Y. J. Kang, *Appl. Mater. Today* **2020**, *19*, 100620; b) R. R. Jia, Y. T. Wang, C. H. Wang, Y. F. Ling, Y. F. Yu, B. Zhang, *ACS Catal.* **2020**, *10*, 3533–3540; c) S. B. Patil, T.-R. Liu, H.-L. Chou, Y.-B. Huang, C.-C. Chang, Y.-C. Chen, Y.-S. Lin, H. Li, Y.-C. Lee, Y. J. Chang, Y.-H. Lai, C.-Y. Wen, D.-Y. Wang, *J. Phys. Chem. Lett.* **2021**, *12*, 8121–8128.
[11] G. Jiang, M. Peng, L. Hu, J. Ouyang, X. Lv, Z. Yang, X. Liang, Y. Liu, H. Liu, *Chem. Eng. J.* **2022**, *435*, 134853.
[12] a) L. Y. Zhang, Z. Y. Wang, J. S. Qiu, *Adv. Mater.* **2022**, *34*, e2109321; b) Y. H. Pei, J. Cheng, H. Zhong, Z. F. Pi, Y. Zhao, F. M. Jin, *Green Chem.* **2021**, *23*, 6975–6983.
[13] L. Yi, Y. Ji, P. Shao, J. Chen, J. Li, H. Li, K. Chen, X. Peng, Z. Wen, *Angew. Chem. Int. Ed.* **2021**, *60*, 21550–21557.
[14] K. X. Yang, N. Zhang, J. F. Yang, Z. Xu, J. Q. Yan, D. Li, S. Z. Liu, *Appl. Catal. B* **2023**, *332*, 122718.
[15] T. Zhao, J. Li, J. Liu, F. Liu, K. Xu, M. Yu, W. Xu, F. Cheng, *ACS Catal.* **2023**, *13*, 4444–4453.
[16] a) X. T. Li, Q. Liu, J. H. Wang, D. C. Meng, Y. J. Shu, X. Z. Lv, B. Zhao, H. Yang, T. Cheng, Q. S. Gao, L. S. Li, H. B. Wu, *Chem* **2022**, *8*, 2148–2162; b) Z. Y. Zhao, X. T. Li, J. H. Wang, X. Z. Lv, H. B. Wu, *J. CO2 Util.* **2021**, *54*, 101741.
[17] Y. Zhou, F. Che, M. Liu, C. Zou, Z. Liang, P. De Luna, H. Yuan, J. Li, Z. Wang, H. Xie, H. Li, P. Chen, E. Bladt, R. Quintero-Bermudez, T.-K. Sham, S. Bals, J. Hofkens, D. Sinton, G. Chen, E. H. Sargent, *Nat. Chem.* **2018**, *10*, 974–980.
[18] K. Yao, J. Li, H. Wang, R. Lu, X. Yang, M. Luo, N. Wang, Z. Wang, C. Liu, T. Jing, S. Chen, E. Cortés, S. A. Maier, S. Zhang, T. Li, Y. Yu, Y. Liu, X. Kang, H. Liang, *J. Am. Chem. Soc.* **2022**, *144*, 14005–14011.
[19] H. Du, H. Guo, K. Wang, X. Du, B. A. Beshiwork, S. Sun, Y. Luo, Q. Liu, T. Li, X. Sun, *Angew. Chem. Int. Ed.* **2022**, *62*, e202215782.
[20] a) M. B. Stevens, C. D. M. Trang, L. J. Enman, J. Deng, S. W. Boettcher, *J. Am. Chem. Soc.* **2017**, *139*, 11361–11364; b) M. Cai, Q. Zhu, X. Wang, Z. Shao, L. Yao, H. Zeng, X. Wu, J. Chen, K. Huang, S. Feng, *Adv. Mater.* **2022**, *35*, 2209338; c) L. Y. Zeng, Y. J. Chen, M. Z. Sun, Q. Z. Huang, K. A. Sun, J. Y. Ma, J. Li, H. Tan, M. G. Li, Y. Pan, Y. Q. Liu, M. C. Luo, B. L. Huang, S. J. Guo, *J. Am. Chem. Soc.* **2023**, *145*, 17577–17587.
[21] L. Yu, L. B. Wu, B. McElhenny, S. W. Song, D. Luo, F. H. Zhang, Y. Yu, S. Chen, Z. F. Ren, *Energy Environ. Sci.* **2020**, *13*, 3439–3446.
[22] a) M. Zhang, J. Guan, Y. C. Tu, S. M. Chen, Y. Wang, S. H. Wang, L. Yu, C. Ma, D. H. Deng, X. H. Bao, *Energy Environ. Sci.* **2020**, *13*, 119–126; b) Z. H. Xiao, C. Lu, J. Wang, Y. Y. Qian, B. W. Wang, Q. Zhang, A. D. Tang, H. M. Yang, *Adv. Funct. Mater.* **2023**, *33*, 2212183.
[23] a) Q. Zhang, I. G. Dalla Lana, K. T. Chuang, H. Wang, *Ind. Eng. Chem. Res.* **2000**, *39*, 2505–2509; b) J. P. Fornés, J. M. Bisang, *Electrochim. Acta* **2017**, *243*, 90–97; c) C. Lyu, Y. Li, J. Cheng, Y. Yang, K. Wu, J. Wu, H. Wang, W. M. Lau, Z. Tian, N. Wang, J. Zheng, *Small* **2023**, *19*, 2302055.
[24] S. Zhang, J. H. Wu, M. T. Zheng, X. Jin, Z. H. Shen, Z. H. Li, Y. J. Wang, Q. Wang, X. B. Wang, H. Wei, J. W. Zhang, P. Wang, S. Q. Zhang, L. Y. Yu, L. F. Dong, Q. S. Zhu, H. G. Zhang, J. Lu, *Nat. Commun.* **2023**, *14*, 3634.
[25] J. Yang, H. F. Qi, A. Q. Li, X. Y. Liu, X. F. Yang, S. X. Zhang, Q. Zhao, Q. K. Jiang, Y. Su, L. L. Zhang, J. F. Li, Z. Q. Tian, W. Liu, A. Q. Wang, T. Zhang, *J. Am. Chem. Soc.* **2022**, *144*, 12062–12071.
[26] R. Daiyan, T. Tran-Phu, P. Kumar, K. Iputera, Z. Tong, J. Leverett, M. H. A. Khan, A. Asghar Esmailpour, A. Jalili, M. Lim, A. Tricoli, R.-S. Liu, X. Lu, E. Lovell, R. Amal, *Energy Environ. Sci.* **2021**, *14*, 3588–3598.
[27] Y. T. Wang, W. Zhou, R. R. Jia, Y. F. Yu, B. Zhang, *Angew. Chem. Int. Ed.* **2020**, *59*, 5350–5354.
[28] J. S. Li, J. F. Gao, T. Z. Feng, H. H. Zhang, D. P. Liu, C. M. Zhang, S. Y. Huang, C. H. Wang, F. Du, C. M. Li, C. X. Guo, *J. Power Sources* **2021**, *511*, 230463.
[29] A. Paliwal, C. D. Bandas, E. S. Thornburg, R. T. Haasch, A. A. Gewirth, *ACS Catal.* **2023**, *13*, 6754–6762.

Manuscript received: July 29, 2023
Revised manuscript received: October 11, 2023
Accepted manuscript online: December 21, 2023
Version of record online: January 30, 2024